



# Spatial Pattern of Precipitation in GPM-Era Satellite Products against Rain Gauge Measurements over Nepal

Bharat Badayar Joshi<sup>1,2</sup>, Munawar Ali<sup>1</sup>, Dibit Aryal<sup>1</sup>, Laxman Paneru<sup>3</sup>, and Bhaskar Shrestha<sup>4,5</sup>\*

<sup>1</sup> Institute of Tibetan Plateau Research, Beijing 100049, China

<sup>2</sup> Kathmandu Center for Research and Education, CAS-TU, Kirtipur, Nepal

<sup>3</sup> Central Department of Hydrology and Meteorology, Tribhuvan University, Kirtipur, Nepal

<sup>4</sup> University of Chinese Academy of Sciences, Beijing 100049, China

<sup>5</sup> State Key Laboratory of Remote Sensing Science, Aerospace Information Research Institute, Chinese Academy of Sciences, Beijing 100049, China

## ARTICLE INFO

Received: 20 March 2021

Received in Revised form: 31 May 2021

Accepted: 3 June 2021

Available Online: 2 December 2021

## Keywords

Satellite Precipitation

IMERG

GSMaP

Nepal

Mountains

\*Correspondence

Bhaskar Shrestha

bhas.stha70@mails.ucas.ac.cn

**Abstract:** Precipitation in a mountainous region is highly variable due to the complex terrain. Satellite-based precipitation estimates are potential alternatives to gauge measurements in these regions, as these typical measurements are not available or are scarce in high elevation areas. However, the accuracy of these gridded precipitation datasets need to be addressed before further usage. In this study, an evaluation of the spatial precipitation pattern in satellite-based precipitation products is provided, including satellite-only (Integrated Multisatellite Retrievals for GPM IMERG-UCORR and Global Satellite Mapping of Precipitation (GSMaP-MVK) and gauge calibrated (IMERG-CORR and GSMaP-Gauge) products, with a spatial resolution of 0.1°, which is compared to 387-gauge measurements in Nepal from April 2014 to December 2016. The major results are as follows: (1) The

gauge calibrated version 5 IMERG-CORR and version 6 GSMaP-Gauge are relatively better than the satellite-only datasets, although they all underestimate the observed precipitation. (2) The daily gauge calibrated GSMaP-Gauge performs fairly well in low and mid-elevation areas, whereas the monthly gauge calibrated IMERG-C performs better in high-elevation areas. (3) For the daily time scale, IMERG-CORR shows a better ability to detect the true precipitation (higher Probability of Detection (POD)) and (lowest False Alarm Ratio (FAR)) events among all datasets. However, all four satellite-based precipitation datasets accurately detect (Critical Success Index (CSI) >40%) precipitation and no-precipitation events. The results of this work provide the systematic quantification of IMERG and GSMaP of satellite precipitation products over Nepal using station observations and delivers a helpful statistical basis for the selection of these datasets for future scientific research.

## 1. Introduction

Precipitation is a fundamental component of the water cycle. Understanding is paramount for managing water systems under a changing climate (Daly *et al.*, 2017; Schneider *et al.*, 2016; Aryal *et al.*, 2020). Mountainous regions play a significant role in regional water resource conservation and sustainable use (Viviroli and Weingartner, 2004). However, these important regions are vulnerable to climate change and several hydro-meteorological hazards, such as floods and landslides. Moreover, the quality and availability of precipitation estimates have a consequential effect on the precision and reliability of meteorological, hydrological, and natural calamities studies (Viviroli *et al.*, 2007; Viviroli *et al.*, 2011).

Nepal is a mountainous country, covering almost 85% of the area by hills and mountains, making the country prone to slope failure causing landslides and debris flows. The Himalayas are water towers and the primary source of many rivers supporting millions of people downstream (Hannah *et al.*, 2005; Sharma *et al.*, 2005; Immerzeel *et al.*, 2020). Precipitation in Nepal is predominantly governed by the summer monsoon system and is highly variable due to complex topography (Krakauer *et al.*, 2013; Hamal *et al.*, 2020a; Hamal *et al.*, 2021). Rain Gauge-based stations provide relatively accurate and actual precipitation measurements at discrete locations on the ground surface (Sun *et al.*, 2018; Hamal *et al.*, 2020c; Sharma *et al.*, 2020c; Sharma *et al.*, 2021b). However, these stations are inadequate for hydro-meteorological studies as their distribution is sporadic. The stations are denser in low lands than high elevation areas (Diodato *et al.*, 2010), leaving the latter underreported estimating precipitation records. Furthermore, the paucity of rain gauge observation hampers comprehensive water management, water resources studies, and the country's discernment of precipitation patterns (Islam *et al.*, 2010). However, high-resolution satellite-based precipitation (SBP) products are the potential alternatives for monitoring precipitation on regular grids nearby. They represent unprecedented measurements over remote areas, especially in a mountainous region where stations are very sparse. However, these estimates are indirect measurements and must be calibrated or verified using gauge observations before further applications (Tian and Peters-Lidard, 2010).

Satellite precipitation estimates are based on one or more remotely-sensed characteristics of clouds, such as reflectivity (Visible), cloud-top temperature (IR

imagery), or from the scattering effect of raindrops particles (i.e., Passive Microwave (PMW) radiation (Hou *et al.*, 2014; Seto *et al.*, 2013; Kidd and Huffman, 2011). Global Precipitation Measurement Core Observation network (GPM-CO) carries a Dual-Frequency Precipitation Radar (DPR) and a multi-channel GPM Microwave Imager (GMI), which has better precipitation measuring capabilities than previous TRMM instruments (Hou *et al.*, 2014). After the success of the Tropical Rainfall Measuring Mission (TRMM), the National Aeronautics and Space Administration (NASA) and the Japanese Aerospace Exploration Agency (JAXA) launched the GPM-CO in February 2014. Two new SBP were introduced after the GPM mission was launched: the Integrated Multi-Satellite Retrievals for GPM (IMERG) and Global Satellite Mapping Precipitation (GSMaP) product of  $0.1^\circ$  spatial resolution, with half-hourly and hourly temporal scales, respectively (Satge *et al.*, 2017). GPM-IMERG takes advantage of several existing precipitation retrieval algorithms, including TRMM Multi-satellite Precipitation Analysis (TMPA), Climate Prediction Center Morphing with Kalman Filter (CMORPH-KF), and Precipitation Estimation from Remotely Sensed Information using Artificial Neural Networks and a Cloud Classification System (PERSIANN-CCS) (Huffman *et al.*, 2017). Meanwhile, GSMaP uses its precipitation retrieving algorithm by assimilating PMW information from GPM Core GMI. PMW based precipitation estimates are more reliable as the observations are analogous to hydrometeorology content present within the atmospheric column (Derin *et al.*, 2016; Huffman *et al.*, 2010; Huffman *et al.*, 2015a). The accuracy of these satellite-based remote sensing precipitation products remains uncertain and poorly investigated, especially in mountainous regions.

Several studies have previously applied SBP products around the globe (Krakauer *et al.*, 2013; Satge *et al.*, 2018; Shen and Xiong, 2016; Tan *et al.*, 2017; Viviroli *et al.*, 2007; Yamamoto *et al.*, 2011; Brown, 2006), and confirmed that newer versions (i.e. V6) of IMERG precipitation datasets are better than its earlier version and previous generation TRMM (Chen and Li, 2016; Prakash *et al.*, 2018; Tang *et al.*, 2016). Further, few studies have been conducted in Nepal using the newer version SBP, whereas critical evaluation of the previous version of SBP (GSMaP, GPM-IMERG) and inter-comparison between these products have not been performed yet. For example, (Bhatt and Nakamura, 2005; Bookhagen and Burbank, 2006) used TRMM precipitation to study precipitation seasonality and diurnal variations over the Himalayas; however, they did not validate the SBP against observations. Yatagai and Kawamoto (2008) found TRMM Precipitation Radar (PR) product underestimated precipitation over the Khumbu area (Himalayan region) of the country. Similarly, (Islam *et al.*, 2010) also found TRMM precipitation product underestimated the observed precipitation; however, they have used only 15 stations for observation data from Nepal without considering geographical variation in the calibration factor. In contrast, (Duncan and Biggs, 2012) indicated that TRMM generally overestimated gauge-based gridded precipitation product (APHRODITE) over Nepal. Studies on spatial comparison with gauge observation found that GSMaP severely underestimated the observed precipitation by about 48 % (Shrestha, 2011).

Moreover, the TRMM 3B-43 precipitation product exhibits reasonable skill in computing precipitation over mountainous Nepal (Krakauer *et al.*, 2013). They also mention that TRMM product shows potentiality for application in water resources management while GSMaP, CMORPH, and PERSIANN were incompetent in

reproducing station precipitation amounts. Recently, (Nepal *et al.*, 2021; Sharma *et al.*, 2020a; Sharma *et al.*, 2020d) have used the latest version (version 6) of GPM-era satellite product for their accuracy. Overall, errors in satellite-based precipitation estimates are partly related to complex topography, underlying surface types, and sensor capability. However, the most recognized and widely used previous versions of satellite products to present the spatial pattern are not analyzed over Nepal. Therefore, this study evaluated the version 5 IMERG (IMERG-CORR, and IMERG-UNCOR) and version 6 GSMaP (GSMaP-MVK, GSMaP-gauge) products for their accuracy and studying the spatial pattern of precipitation over Nepal. The evaluated datasets include both gauge-calibrated and un-calibrated GPM-IMERG and GSMaP products.

## 2. Materials and Methods

### 2.1 Study Area

Nepal is a South Asian country located approximately between 26.36° – 30.45°N latitude and 80.06° – 88.2°E longitude (Figure 1). It encompasses the northern part of the Indo-Gangetic plains and the southern part of the high Himalayan range covering 147,516 km<sup>2</sup>. About 85 % of the country is comprised of hilly and mountainous regions, with the remaining 14 % as flatland (Chen *et al.*, 2021). Its topography varies from almost 60 m in the southern lowland to the world's highest peak, i.e., Mt. Everest, at an altitude of 8848.86 m above sea level, in the north within a short distance of ~150-200 km. The geography of the country is broadly divided into Lowlands (Terai and Siwaliks), Hills (Middle and High Mountains), and High Himalayas (Duncan and Biggs, 2012). The country's climate is very diverse in space and seasons, which is governed by south Asian summer monsoons and a westerly wind system. Pre-monsoon (March-May), summer monsoon (June-September), post-monsoon (October-November), and winter seasons (December-February) are the primary climatological seasons (Nayava, 1980). Among these seasons, post-monsoon and winter seasons are generally dry. In contrast, the pre-monsoon and monsoon seasons are wet and humid (Shrestha, 2000; Sharma *et al.*, 2021a). Low-land and Mid-Mountains receive large amounts of precipitation during the summer monsoon from July to September as part of the South Asian monsoon, which is the country's primary source of annual precipitation (Hamal *et al.*, 2020a; Hamal *et al.*, 2020b; Hamal *et al.*, 2020c; Sharma *et al.*, 2020b; Shrestha and Deshar, 2014; Shrestha *et al.*, 2021). Meanwhile, the northern part of the high Himalayas, including trans-Himalayan regions, is relatively dry as mountains block the precipitation and are known as rain shadow areas (Dawadi *et al.*, 2020; Pokharel *et al.*, 2019; Talchabhadel and Karki, 2019; Talchabhadel *et al.*, 2018).

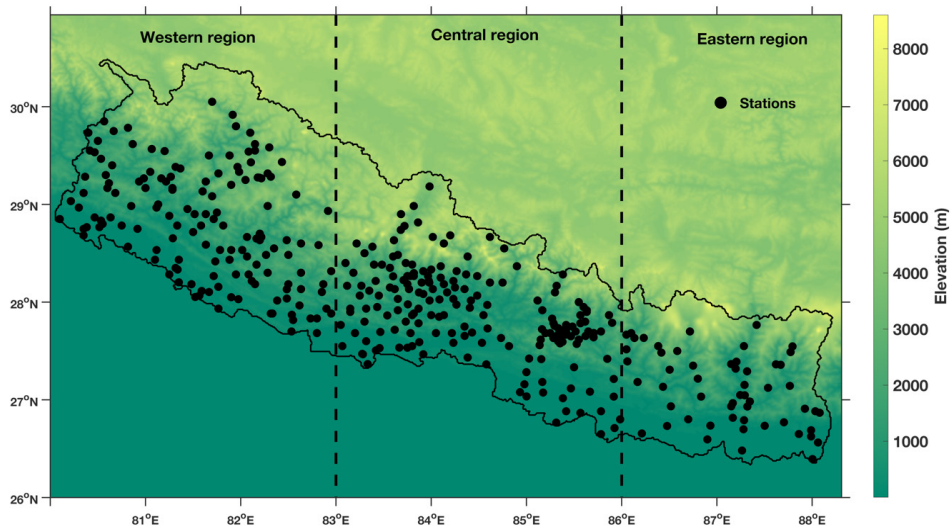


**Figure 1.** Study area Nepal and distribution of 387 meteorological stations.

## 2.2 Ground Data

This study used daily rainfall data of 387 stations across Nepal from April 2014 to 2016 (Figure 1). This data was collected from the Department of Hydrology and Meteorology (DHM), the Government of Nepal that owns the hydro-meteorological station and is responsible for data collection. The distribution of these rain gauge stations is very erratic. Most of the stations are located in mid, and low-altitude regions, and existing stations in higher altitudes are inadequate to represent the precipitation variability of the country. Most of these stations are manual-type, therefore subject to personnel and instrumental errors. The mean annual precipitation of selected individual rain gauge stations during the study period is presented in Figure 2a.

## 2.3 Satellite datasets

IMERG is the global multi-satellite precipitation product developed by National Aeronautic Space Agency (NASA). It combines the infrared (IR) satellite estimates, microwave (MW) precipitation estimates and is finally adjusted by monthly gauge observation from the Global Precipitation Climatology Centre (GPCC) (Huffman *et al.*, 2015b; Huffman *et al.*, 2017). The IMERG system runs three times, Early, Late, and Final Run. The Early Run product provides a preliminary estimate after 4hrs of the observation time, while the Late Run product is available after 12hrs of observation time. The Final Run product combines Late Run and gauges observation, which is available after 2.5 months of observation time (Huffman *et al.*, 2017). Among these three IMERG products, Final Run is mainly recommended for Research purposes (Tan *et al.*, 2017; Huffman *et al.*, 2015b). There are two precipitation data field variables embedded in the Final Run product: monthly GPCC gauge calibrated multi-satellite precipitation

estimated as a "precipitationCal" (hereafter IMERG-CORR) and the original multi-satellite precipitation estimate "precipitationUncal" (hereafter IMERG-UNCOR). For this study, Half hourly Final Run version 5B IMERG-UNCOR and IMERG-CORR with spatial resolution of 10km from April 2014 to December 2016 were acquired from the PMW website (<https://gpm.nasa.gov/data-access/downloads/gpm>).

GSMaP is a satellite-based precipitation product of the Japan Science and Technology (JST) agency under the Core Research for Evolutional Science and Technology (CREST) (Satge *et al.*, 2018). GSMaP combines various available PMW and IR sensors (Shige *et al.*, 2009). While developing GSMaP precipitation product, the instantaneous precipitation rate is retrieved based on the PMW radiometers from different satellite platforms, including GMI, advanced microwave scanning radiometer 2 (AMSR2), TRMM Microwave Imager (TMI), special sensor microwave imager/sounder (SSMIS), advanced microwave sounding unit-A (AMSU-A), and microwave humidity sounder (MHS). Subsequently, the gaps between PMW-based estimates are propagated using the cloud motion vectors computed from geo-IR images, and a Kalman filter approach is applied to refine the precipitation rate (Ushio *et al.*, 2009). Finally, forward, and backward propagated precipitation estimates are weighted and combined to generate the GSMaP-MVK product (Hou *et al.*, 2014).

GSMaP-MVK also uses IR to correct satellite estimates but adopts various PWM imagers and sounders; it has a latency of 3 days. In addition to PWM and IR, GSMaP-Gauge is a gauge-calibrated product that adjusts the GSMaP-MVK estimate with National Oceanic and Atmospheric Administration (NOAA)/Climate Prediction Center (CPC) gauge-based analysis of global daily precipitation biases with a latency of 3 days. In the current study, version 6 GSMaP-MVK and GSMaP-Gauge (V06) were used. Mean annual precipitation during the study period of all SBPs is presented in Figure 2. An overview of the details of datasets is provided in Table 1.

**Table 1.** Overview of datasets included in this study with the corresponding spatial resolution, temporal coverage.

Product	Temporal Resolution	Spatial Resolution	Period	Coverage	References
DHM (gauge observation)	1 day	387 stations	2014.04–2016.12	Within Nepal	<a href="http://www.dhm.gov.np">www.dhm.gov.np</a>
IMERG-UNCOR	0.5h	0.1°	2014.04–2016.12	90° N–90° S	(Huffman <i>et al.</i> , 2019).
IMERG-CORR	0.5h	0.1°	2014.04–2016.12	90° N–90° S	
GSMaP-MVK	1h	0.1°	2014.04–2016.12	60° N–60° S	(Satge <i>et al.</i> , 2018)
GSMaP-Gauge	1h	0.1°	2014.04–2016.12	60° N–60° S	

## 2.4 Methodology

All SBPs precipitation products were extracted using the location of the observed gauge station (point-pixel method). Daily temporal datasets are computed using sub-daily SBP to match the time window of daily gauges observations for each station. Some of the gauge observation contains a missing value; thus, quality control is applied for data consistency. Accordingly, if the station featured more than 80% daily data in a month, it is averaged for monthly value; otherwise, precipitation is considered

a missing value. To make consistent datasets, if there is a missing value in observation, SBP datasets were also considered missing values.

For each station, annual precipitation values of SBP and observation were generated by averaging monthly precipitation. To quantify spatial pattern in SBP, stations were divided into three different elevation sections, i.e., low-elevation (all stations below 1500 m), mid-elevation (station located between 1500 and 2500 m), and high-elevation (stations situated above 2500 m) regions. Further, precipitation values were averaged at each station to quantify the performance of SBPs. Furthermore, precipitation detection capability of each SBP were calculated at each station along with the observation.

### 2.4.1 Statistical analysis

Following the previous studies (Hamal et al., 2020c; Sharma et al., 2020a; Shrestha et al., 2021), four different statistical metrics are adopted to analyze the performance of four SBP products: correlation coefficient (CC, Equation 1), Normalized Root Mean Square Error (NRMSE, Equation 2), mean biases (MB, Equation 3), and absolute relative error (RE, Equation 4). CC measures the strength and direction of the linear association between SBP and observation, while NRMSE provides the averaged magnitude of the deviation of SBP from observation. Furthermore, MB and RE show the average bias (underestimation or overestimation) and the difference between the magnitude of the SBP with observation, respectively.

$$CC = \frac{\sum_{i=1}^n (G_i - \bar{G})(S_i - \bar{S})}{\sqrt{\sum_{i=1}^n (G_i - \bar{G})^2} \sqrt{\sum_{i=1}^n (S_i - \bar{S})^2}} \quad (1)$$

$$NRMSE = \frac{\sqrt{\sum_{i=1}^n (S_i - G_i)^2}}{\bar{G}} \quad (2)$$

$$MB = \frac{(\bar{S} - \bar{G})}{n} \quad (3)$$

$$RE = \left| \frac{MB}{\bar{G}} \right| \quad (4)$$

\*Where G is gauge observation, S is the SBPs, and n denotes the sample size.

Additionally, three skill indices are calculated at each station based on a 2x2 contingency table (Table 2) of daily rain/no-rain events. Since most DHM observations are collected manually, the threshold value for rain events is considered 1mm/day. In Table 2, Q1 represents correctly estimated rain events of observation by SBP, Q2 and Q3 represent a false estimation of rain and no-rain event by SBP when there is no-rain and rain event in gauge observed data, respectively. Q4 refers to correctly estimated no-rain events by SBP. Skill indices - Probability of Detection (POD), also known as hit-rate, measures the fraction of the correctly diagnosed gauge observed events. False Alarm Ratio (FAR) gives the fraction of diagnosed events that did not occur, and Critical

Success Index (CSI) measures how well SBP corresponds to gauge observed data that were corrected. The formula of statistical matrices is as follows.

$$POD = \frac{Q1}{(Q1+Q3)} \quad (5)$$

$$FAR = \frac{Q2}{(Q1+Q2)} \quad (6)$$

$$CSI = \frac{Q1}{Q1+Q2+Q3} \quad (7)$$

Where Q1, Q2, Q3, and Q4 are the possible events shown in Table 2.

**Table 2.** Contingency Table to define daily precipitation based categorical scores for the evaluation of SBP with gauge observation.

Gauges			
SBP	Precipitation No Precipitation	Precipitation	No Precipitation
		Q1	Q2
		Q3	Q4

### 3. Results

#### 3.1 Spatial performance

Figure 2(a through e) shows the spatial distribution of the mean annual precipitation (mm/day) derived from the observed data and four different SBP datasets averaged for the study period. Comparing the spatial distributions of the observed precipitation, all four SBP datasets captured general spatial patterns, i.e., the highest amount of precipitation in the central Nepal. However, they differ largely in the precipitation amount and location accuracy. The observed maximum precipitation is more than 10 mm/day and centred at approximately 28.3° N, 84° E (Figure 2a). The annual precipitation distribution from GSMaP-Gauge (Figure 2e) shows similar characteristics with the maximum precipitation (approximately 8-10 mm/day) at 28.3° N, 84° E, whereas GSMaP-MVK shows the maximum precipitation (approximately 3-4 mm/day) at 28.5° N, 84° E (Figure 2b). In contrast, the IMERG-UNCORR and IMERG-CORR datasets show the maximum precipitation (approximately 6-8 mm/day) at 27.8° N, 84.7° E (Figures 2a and c). Overall, all four SBP datasets tend to underestimate the annual precipitation across the country. The estimated spatial pattern by GSMaP-Gauge (Figure 2e) is close to the observed dataset followed by IMERG-UNCOR (Figure 2b), and then IMERG-CORR (Figure 2d), whereas GSMaP-MVK (Figure 2c) shows the most dissimilarity with the observation.

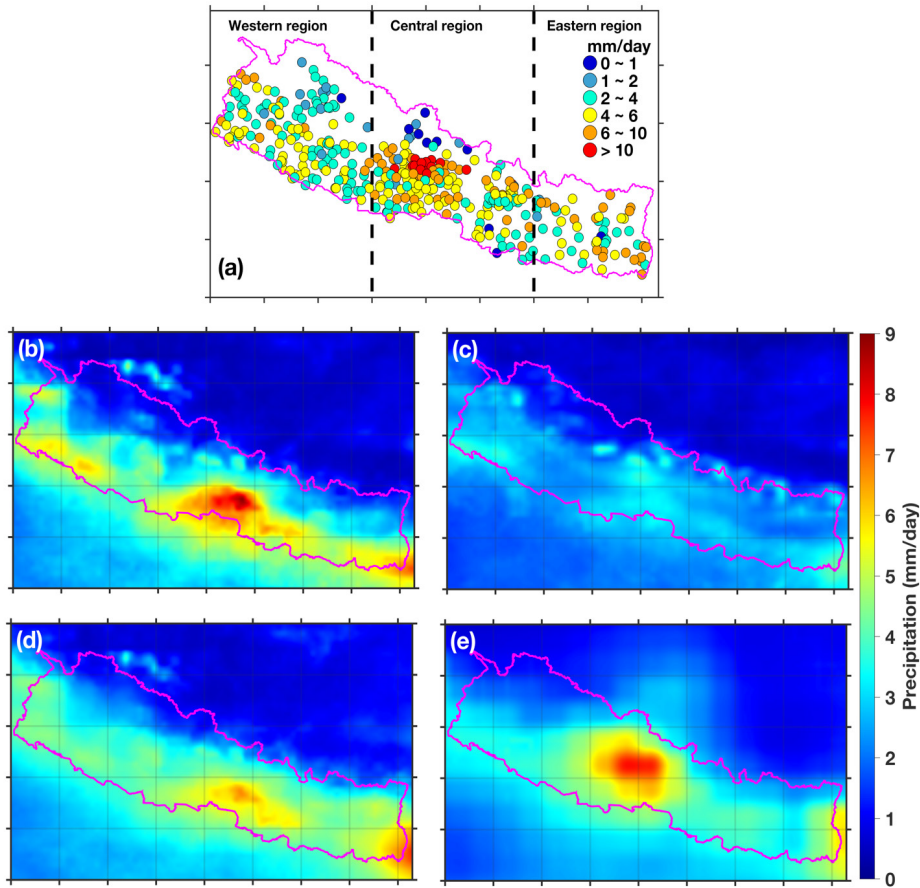


**Figure 2.** Spatial patterns of daily average precipitation (mm/day) in (a) observation, (b) IMERG-UNCOR, (c) GSMaP-MVK, (d) IMERG-CORR, and (e) GSMaP-Gauge from April 2014 to 2016.

To quantify the performances of SBPs at different elevation sections, we have compared all four SBP at three different elevations sections. Table 3 shows the statistical metrics derived from mean monthly precipitation averaged over below 1500 m, between 1500 and 2500 m, and above 2500 m elevation, respectively. The negative MB values in table 3 demonstrate that all four SBP underestimated the observed precipitation at below 1500 m elevation. It is noteworthy that GSMaP-Gauge effectively reduces the systematic errors (30 % of RE) of GSMaP-MVK with bias-correction using the daily CPC gauge-based observation, which is only 2.6 % when GPCC monthly gauge-analysis used in IMERG data set. The CC values in IMERG-UNCORR and GSMaP-MVK are 0.14 and 0.58, respectively, which is 0.3 and 0.6 in IMERG-CORR and GSMaP-Gauge (Table 3).

**Table 3.** Statistical metrics in low-elevation (below-1500 m), mid-elevation (between 1500 and 2500 m), and high-elevation (above 2500 m), as well as in the national scale. Values are calculated by averaging the precipitation values at each station.

Regions	Datasets	Mean (mm/day)	MB (mm/day)	NRMSE	CC	RE (%)
Below 1500 m	IMERG-UNCORR	4.33	<b>-0.54</b>	0.55	0.14	<b>11.01</b>
	IMERG-CORR	4.2	-0.67	<b>0.5</b>	0.3	13.68
	GSMaP-MVK	2.63	-2.23	0.64	0.58	45.9
	GSMaP-Gauge	4.1	-0.77	0.43	<b>0.6</b>	15.79
Between 1500-2500 m	IMERG-UNCORR	3.1	-2.35	0.69	0.29	43.13
	IMERG-CORR	3.75	-1.7	0.6	0.37	31.22
	GSMaP-MVK	2.29	-3.16	0.76	0.71	58.05
	GSMaP-Gauge	3.96	<b>-1.49</b>	<b>0.48</b>	<b>0.72</b>	<b>27.3</b>
Above 2500 m	IMERG-UNCORR	1.69	-1.07	0.98	0.36	38.83
	IMERG-CORR	2.22	<b>-0.55</b>	<b>0.82</b>	<b>0.69</b>	<b>19.79</b>
	GSMaP-MVK	1.6	-1.16	0.97	0.51	42.06
	GSMaP-Gauge	3.4	0.64	1.2	-0.09	22.96
National Scale	IMERG-UNCORR	3.85	-1.01	0.61	0.2	20.81
	IMERG-CORR	3.96	-0.91	0.54	0.37	18.69
	GSMaP-MVK	2.48	-2.39	0.69	<b>0.59</b>	49.06
	GSMaP-Gauge	4.02	<b>-0.85</b>	<b>0.48</b>	0.58	17.44

The MB and NRMSE were higher in IMERG products, whereas CC was higher in GSMaP products except above 2500 m. The result further indicates that in lowland with moderate precipitation, IMERG products are more consistent with estimating the precipitation amount (smaller MB), while GSMaP products can better represent the spatial distribution (higher CC) of observed precipitation. In a mid-elevation region characterized by high precipitation, GSMaP-Gauge performs reasonably well with lower MB (-1.49 mm/day), NRMSE (0.48), and higher CC (0.72) among all SBP. Meanwhile, CC-value is very similar between GSMaP-MVK and GSMaP-Gauge. In this region, IMERG products are less capable of representing the spatial pattern (lower CC-value) even after the GPCP gauge calibration. Systematic errors are significantly improved (reduced RE) after the gauge calibration in both IMERG-CORR and GSMaP-Gauge at mid and low-elevation areas.

Further, in high-elevation areas with complex terrain and low precipitation, gauge calibrated IMERG-CORR underestimated, and GSMaP-Gauge overestimated mean monthly precipitation with similar MB of -0.55 and 0.64 mm/day, respectively. Overall, at national scale, GSMaP-Gauge outperforms all SBPs indicating that GSMaP-Gauge shows better overall performance followed by IMERG-CORR, IMERG-UNCORR and GSMaP-MVK.

### 3.2 Precipitation detection capability

To analyze the precipitation detection capability of four SBPs, POD, FAR and CSI is calculated at each station and presented in Figure 3. All SBP products under the study showed an overall good performance, with the IMERG-CORR showing the best performance with a POD higher than 70% at each station (Figure 3d), followed by GSMaP-Gauge (POD > 65%) (Figure 3j). Both gauge calibrated products show good performance compared to the un-calibrated versions in detecting the observed precipitation events. In general, the SBPs products had the high capability to correctly estimate overall rain and no-rain events (CSI < 40%) (Figure 3c, f, i and l). Among them, both un-calibrated datasets show similar CSI (~40%), where IMERG-CORR had better capability to detect rain and no-rain events (CSI < 30%) (Figure 3f). Further, IMERG-CORR also showed the lowest FAR among all SBPs, indicating only about 40% of estimated precipitation at most of the stations when there is no rainfall from observed data (Figure 3e). Again, both un-corrected versions showed a similar capability to detect false precipitation events; however, the difference is small.

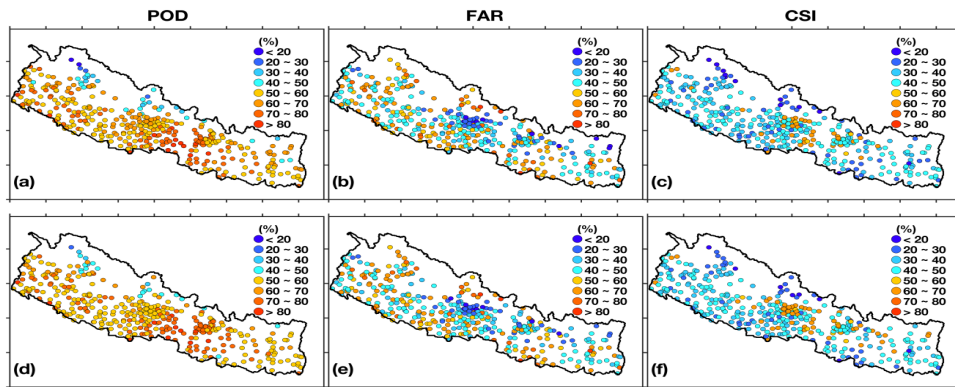


**Figure 3.** Precipitation detection capability of (a,d,g,h) POD, (b,e,j,k) FAR and (c,f,i,l) CSI for IMERG-UNCORR (first row: a,b,c), IMERG-CORR (second row: d,e,f), GSMaP-MVK (third row: g,h,i) and GSMaP-Gauge (forth row: j,k,l) during the study period.

## 4. Discussion

SBP products are potential alternatives for estimating precipitation - where there is no representation of gauge data, which creates new opportunities for hydro-meteorological phenomena in understanding and applying remotely-sensed information. In this study, we presented spatial performance of four satellite-based precipitation datasets from the GPM-era SBP (GPM-IMERG and GSMaP) product with the gauge observations from Nepal. In all four SBP datasets, GSMaP-Gauge has the best overall performance, followed by IMERG-CORR, IMERG-UNCORR, and GSMaP-MVK. Several previous studies have also found that gauge-calibrated SBP generally show higher accuracy than their satellite-only versions due to observed gauge adjustment on these datasets (Sungmin *et al.*, 2017; Wang *et al.*, 2017; Yuan *et al.*, 2019). However, precipitation estimates from IMERG-C and GSMaP-Gauge largely depend on the gauge-based GPCC and CPC data set, respectively. If the gauge-based data set represents precipitation estimates better in a region, then these gauge-calibrated SBP datasets will also show remarkable scores in this region. Thus, quality calibrated gauge datasets remarkably influence the accuracy of the IMERG-C, and GSMaP-Gauge precipitation estimates.

GPM-IMERG precipitation products are based on PMW and IR sensors available from Low Earth Orbital (LEO) and geostationary satellites. It also uses the datasets of surface temperature, relative humidity, and surface pressure provided by European Centre for Medium-Range Weather Forecasts (Huffman *et al.*, 2017; Zhao *et al.*, 2018). IMERG-UNCORR is satellite-only datasets where IMERG-CORRR was corrected using GPCC monthly precipitation-based coefficients. In comparison with satellite-only and gauge calibrated IMERG datasets, as expected, gauge calibrated IMERG-CORR systematically provides a more realistic precipitation estimate than its corresponding satellite-only (IMERG-UNCORR) data set (see Figure 2 and Table 3). IMERG-CORR significantly improved the performance based on a monthly timescale as this precipitation estimate is strongly dependent on the GPCC gauge calibration. On the other hand, slightly improved performance on the daily time scale is more dependent on other components of the algorithms. Therefore, IMERG precipitation improvement at the daily timescale is a reflection of IMERG algorithms (Satge *et al.*, 2018). Interestingly, both of the IMERG datasets had a weak correlation in low and mid-elevation areas as compared to the GSMaP product. Therefore, it can be assessed that the IMERG algorithm and error-correction method are more effective in balancing errors at high-elevation areas or for low precipitation rates (Sharma *et al.*, 2020a). This reveals that IMERG precipitation products are less reliable to detect higher precipitation rates.

Regarding GSMaP products, GSMaP-MVK largely underestimated the mean annual precipitation over the country, but, the negative bias was significantly reduced in GSMaP-Gauge, which was calibrated with CPC daily gauge data. Both of these datasets well captured the spatial pattern of precipitation over the country. Therefore, the algorithms used in GSMaP product are more proficient at capturing the spatial pattern of observed precipitation than those used in IMERG. Meanwhile, the relatively weaker performance of GSMaP-Gauge in high-elevation with lower precipitation rate might be related to quality of assembled gauge observation in CPC datasets. In general, the considerable underestimation for gauge-adjusted datasets may be attributed to

the sparse, unevenly spaced gauge stations and the optimal interpolation technique. Another reason might be subjected to the fact that both PMW and IR satellites have difficulty detecting shallow orographic precipitation (Derin *et al.*, 2016; Satge *et al.*, 2018; Ushio *et al.*, 2009). Thus, it seems important to calibrate satellite-based precipitation estimates at different rain rates and higher elevations.

However, SBP are indirect measurements that are based on satellite/sensor constellations, including PMW and IR sensors onboard LEO and geosynchronous satellites, and are subjected to uncertainty due to technical limitations (Sharma *et al.*, 2020a; Sharma *et al.*, 2020d). Indeed, the irregular sampling and limited overpass of LEO PMW measurements impede the correct capture of short-term, and slight precipitation events. We also found that the complex terrain and strong local convective weather significantly influence the satellite rainfall retrieval and result in unexpected errors between satellite estimates and gauge observations.

## 5. Conclusion

This study attempts to evaluate the spatial pattern of precipitation in version 5 IMERG and version 6 GSMaP products, including satellite-only (IMERG-UNCORR and GSMaP-MVK) and gauge calibrated (IMERG-CORR and GSMaP-Gauge) products, against 387-gauge measurements in Nepal from April 2014 to December 2016. Conventional statistical metrics and evaluation scores were used to quantify the performances of these SBPs.

The precipitation amount in SBPs differs significantly, depending on the location. All four SBP datasets underestimated the observed precipitation over Nepal. However, all four datasets can capture the main spatial precipitation pattern (highest precipitation concentrated over mid-elevation areas of the central region). The precipitation estimated from both gauge calibrated SBP (IMERG-CORR and GSMaP-Gauge) datasets were better than that estimated from satellite-only (IMERG-UNCORR and GSMaP-MVK) datasets. In low and mid-elevation areas (below 2500 m) with relatively high precipitation, GSMaP-Gauge performs best in estimating precipitation amount and reflecting the observed spatial patterns among the four datasets. However, in high-elevation areas (above 2500 m) with complex topography, IMERG-CORR shows smaller MB and RRMSE values and higher R values than GSMaP-Gauge, IMERG-UNCORR, and GSMaP-MVK.

During the study period, when we choose 1 mm/day as the threshold of the daily rainfall event, IMERG product shows a better ability to detect actual precipitation (higher POD) than GSMaP product. IMERG-CORR shows the best performance for detecting no-precipitation events (lowest FAR scores) among the selected datasets. However, all four SBPs accurately detect (CSI <40%) precipitation and no-precipitation events across the country.

The present work fills the gap of the lack of a systematic evaluation for the four GPM-Era SBPs in Nepal. This comprehensive evaluation delivers a statistical basis and provides a concrete outlook on data selection in meteorological, hydrological, glaciological, and disaster-related studies within the study region.

**Acknowledgments:** The authors express their sincere thanks to the scientists at the NASA and JAXA, who were responsible for the development of the IMERG and GSMaP algorithms and for providing satellite precipitation data. The DHM and the government of Nepal are also acknowledged for providing the observed precipitation datasets. The authors express their gratitude to Mr. Shankar Sharma for providing valuable suggestions and help for the study.

**Conflicts of Interest:** The authors declare no conflict of interest.

## References

- Aryal, D., Wang, L., Adhikari, T. R., Zhou, J., Li, X., Shrestha, M., Wang, Y. and Chen, D. (2020) A Model-Based Flood Hazard Mapping on the Southern Slope of Himalaya. *Water*, **12**: 540. <https://doi.org/10.3390/w12020540>
- Bhatt, B. C. and Nakamura, K. (2005) Characteristics of monsoon rainfall around the Himalayas revealed by TRMM precipitation radar. *Monthly Weather Review*, **133**: 149-165. <https://doi.org/10.1175/Mwr-2846.1>
- Bookhagen, B. and Burbank, D. W. (2006) Topography, relief, and TRMM-derived rainfall variations along the Himalaya. *Geophysical Research Letters*, **33**. Art. L08405. <https://doi.org/10.1029/2006gl026037>.
- Brown, J. E. (2006) An analysis of the performance of hybrid infrared and microwave satellite precipitation algorithms over India and adjacent regions. *Remote Sensing of Environment*, **101**: 63-81.
- Chen, F. R. and Li, X. (2016) Evaluation of IMERG and TRMM 3B43 Monthly Precipitation Products over Mainland China. *Remote Sensing*, **8**.
- Chen, Y., Sharma, S., Zhou, X., Yang, K., Li, X., Niu, X., Hu, X. and Khadka, N. (2021) Spatial performance of multiple reanalysis precipitation datasets on the southern slope of central Himalaya. *Atmospheric Research*, **250**: 105365. <https://doi.org/10.1016/j.atmosres.2020.105365>
- Daly, C., Slater, M. E., Roberti, J. A., Laseter, S. H. and Swift, L. W. (2017) High-resolution precipitation mapping in a mountainous watershed: ground truth for evaluating uncertainty in a national precipitation dataset. *International Journal of Climatology*, **37**: 124-137. <https://doi.org/10.1002/joc.4986>
- Dawadi, B., Saroj, R. H. A. D. L., Ishwar, P. and Shrestha, K. (2020) A Short Note on Linkage of Climatic Records between Terai and Mid-mountain of Central Nepal. *Journal of Geographical Research* | Volume, **3**.
- Derin, Y., Anagnostou, E., Berne, A., Borga, M., Boudevillain, B., Buytaert, W., Chang, C. H., Delrieu, G., Hong, Y., Hsu, Y. C., Lavado-Casimiro, W., Manz, B., Moges, S., Nikolopoulos, E. I., Sahlu, D., Salerno, F., Rodriguez-Sanchez, J. P., Vergara, H. J. and Yilmaz, K. K. (2016) Multiregional Satellite Precipitation Products Evaluation over Complex Terrain. *Journal of Hydrometeorology*, **17**: 1817-1836.
- Diodato, N., Tartari, G. and Bellocchi, G. (2010) Geospatial Rainfall Modelling at Eastern Nepalese Highland from Ground Environmental Data. *Water Resources Management*, **24**: 2703-2720. <https://doi.org/10.1007/s11269-009-9575-2>
- Duncan, J. M. and Biggs, E. M. (2012) Assessing the accuracy and applied use of satellite-derived precipitation estimates over Nepal. *Applied Geography*, **34**: 626-638.
- Hamal, K., Khadka, N., Rai, S., Joshi, B. B., Dotel, J., Khadka, L., Bag, N., Ghimire, S. K. and Shrestha, D. (2020a) Evaluation of the TRMM Product for Spatio-temporal Characteristics

- of Precipitation over Nepal (1998-2018). *Journal of Institute of Science and Technology*, **25**: 39-48.
- Hamal, K., Sharma, S., Baniya, B., Khadka, N. and Zhou, X. (2020b) Inter-Annual Variability of Winter Precipitation Over Nepal Coupled With Ocean-Atmospheric Patterns During 1987–2015. *Frontiers in Earth Science*, **8**: 161. <https://doi.org/10.3389/feart.2020.00161>
- Hamal, K., Sharma, S., Khadka, N., Baniya, B., Ali, M., Shrestha, M. S., Xu, T., Shrestha, D. and Dawadi, B. (2020c) Evaluation of MERRA-2 Precipitation Products Using Gauge Observation in Nepal. *Hydrology*, **7**: 40. <https://doi.org/10.3390/hydrology7030040>
- Hamal, K., Sharma, S., Pokharel, B., Shrestha, D., Talchabhadel, R., Shrestha, A. and Khadka, N. (2021) Changing pattern of drought in Nepal and associated atmospheric circulation. *Atmospheric Research*: 105798.
- Hannah, D. M., Kansakar, S. R., Gerrard, A. J. and Rees, G. (2005) Flow regimes of Himalayan rivers of Nepal: nature and spatial patterns. *Journal of Hydrology*, **308**: 18-32. [10.1016/j.jhydrol.2004.10.018](https://doi.org/10.1016/j.jhydrol.2004.10.018)
- Hou, A. Y., Kakar, R. K., Neeck, S., Azarbarzin, A. A., Kummerow, C. D., Kojima, M., Oki, R., Nakamura, K. and Iguchi, T. (2014) The Global Precipitation Measurement Mission. *Bulletin of the American meteorological Society*, **95**: 701+. [10.1175/Bams-D-13-00164.1](https://doi.org/10.1175/Bams-D-13-00164.1)
- Huffman, G. J., Adler, R. F., Bolvin, D. T. and Nelkin, E. J. 2010. The TRMM Multi-Satellite Precipitation Analysis (TMPA). In *Satellite Rainfall Applications for Surface Hydrology*, Gebremichael, M. and Hossain, F. (eds.). Springer Netherlands: Dordrecht; 3-22.
- Huffman, G. J., Bolvin, D. T., Braithwaite, D., Hsu, K., Joyce, R., Xie, P. and Yoo, S.-H. (2015a) NASA global precipitation measurement (GPM) integrated multi-satellite retrievals for GPM (IMERG). *Algorithm Theoretical Basis Document (ATBD) Version*, **4**: 26.
- Huffman, G. J., Bolvin, D. T., Braithwaite, D., Hsu, K., Joyce, R., Xie, P. and Yoo, S.-H. (2019) NASA global precipitation measurement (GPM) integrated multi-satellite retrievals for GPM (IMERG). *Algorithm Theoretical Basis Document (ATBD) Version 06*, **6**: 26.
- Huffman, G. J., Bolvin, D. T. and Nelkin, E. J. (2015b) Integrated Multi-satellitE Retrievals for GPM (IMERG) technical documentation. *NASA/GSFC Code*, **612**: 47.
- Huffman, G. J., Bolvin, D. T. and Nelkin, E. J. (2017) Integrated Multi-satellitE Retrievals for GPM (IMERG) technical documentation. *NASA/GSFC Code*, **612**: 47.
- Immerzeel, W. W., Lutz, A., Andrade, M., Bahl, A., Biemans, H., Bolch, T., Hyde, S., Brumby, S., Davies, B. and Elmore, A. (2020) Importance and vulnerability of the world's water towers. *Nature*, **577**: 364-369.
- Islam, M., Das, S. and Uyeda, H. (2010) Calibration of TRMM derived rainfall over Nepal during 1998-2007. *The Open Atmospheric Science Journal*, **4**.
- Kidd, C. and Huffman, G. (2011) Global precipitation measurement. *Meteorological Applications*, **18**: 334-353.
- Krakauer, N. Y., Pradhanag, S. M., Lakhankar, T. and Jha, A. K. (2013) Evaluating Satellite Products for Precipitation Estimation in Mountain Regions: A Case Study for Nepal. *Remote Sensing*, **5**: 4107-4123. <https://doi.org/10.3390/rs5084107>
- Nayava, J. L. (1980) Rainfall in Nepal. *Himalayan Review*, **12**: 1-18.
- Nepal, B., Shrestha, D., Sharma, S., Shrestha, M. S., Aryal, D. and Shrestha, N. (2021) Assessment of GPM-Era Satellite Products' (IMERG and GSMaP) Ability to Detect Precipitation Extremes over Mountainous Country Nepal. *Atmosphere*, **12**: 254.
- Pokharel, B., Wang, S. Y. S., Meyer, J., Marahatta, S., Nepal, B., Chikamoto, Y. and Gillies, R. (2019) The east–west division of changing precipitation in Nepal. *International Journal of Climatology*, **40**: 3348-3359. <https://doi.org/10.1002/joc.6401>

- Prakash, S., Mitra, A. K., AghaKouchak, A., Liu, Z., Norouzi, H. and Pai, D. S. (2018) A preliminary assessment of GPM-based multi-satellite precipitation estimates over a monsoon dominated region. *Journal of Hydrology*, **556**: 865-876.
- Satge, F., Hussain, Y., Bonnet, M. P., Hussain, B. M., Martinez-Carvajal, H., Akhter, G. and Uagoda, R. (2018) Benefits of the Successive GPM Based Satellite Precipitation Estimates IMERG-V03,-V04,-V05 and GSMaP-V06,-V07 Over Diverse Geomorphic and Meteorological Regions of Pakistan. *Remote Sensing*, **10**.
- Satge, F., Xavier, A., Zola, R. P., Hussain, Y., Timouk, F., Garnier, J. and Bonnet, M. P. (2017) Comparative Assessments of the Latest GPM Mission's Spatially Enhanced Satellite Rainfall Products over the Main Bolivian Watersheds. *Remote Sensing*, **9**. UNSP 369, <https://doi.org/10.3390/rs9040369>
- Schneider, U., Ziese, M., Meyer-Christoffer, A., Finger, P., Rustemeier, E. and Becker, A. (2016) The new portfolio of global precipitation data products of the Global Precipitation Climatology Centre suitable to assess and quantify the global water cycle and resources. *Water Resources Assessment and Seasonal Prediction*, **374**: 29-34. 10.5194/piahs-374-29-2016
- Seto, S., Iguchi, T. and Oki, T. (2013) The Basic Performance of a Precipitation Retrieval Algorithm for the Global Precipitation Measurement Mission's Single/Dual-Frequency Radar Measurements. *Ieee Transactions on Geoscience and Remote Sensing*, **51**: 5239-5251.
- Sharma, S., Bajracharya, R. M., Sitaula, B. K. and Merz, J. (2005) Water quality in the Central Himalaya. *Current Science*, **89**: 774-786.
- Sharma, S., Chen, Y., Zhou, X., Yang, K., Li, X., Niu, X., Hu, X. and Khadka, N. (2020a) Evaluation of GPM-Era Satellite Precipitation Products on the Southern Slopes of the Central Himalayas Against Rain Gauge Data. *Remote Sensing*, **12**: 1836. <https://doi.org/10.3390/rs12111836>
- Sharma, S., Hamal, K., Khadka, N., Ali, M., Subedi, M., Hussain, G., Ehsan, M. A., Saeed, S. and Dawadi, B. (2021a) Projected Drought Conditions over Southern Slope of the Central Himalaya Using CMIP6 Models. *Earth Systems and Environment*: 1-11. <https://doi.org/10.1007/41748-021-00254-1>
- Sharma, S., Hamal, K., Khadka, N. and Joshi, B. B. (2020b) Dominant pattern of year-to-year variability of summer precipitation in Nepal during 1987–2015. *Theoretical and applied climatology*, **142**: 1071-1084. <https://doi.org/10.1007/s00704-020-03359-1>
- Sharma, S., Khadka, N., Hamal, K., Baniya, B., Luintel, N. and Joshi, B. B. (2020c) Spatial and Temporal Analysis of Precipitation and Its Extremities in Seven Provinces of Nepal (2001-2016). *Applied Ecology and Environmental Sciences*, **8**: 64-73. <https://doi.org/10.12691/aees-8-2-4>
- Sharma, S., Khadka, N., Hamal, K., Shrestha, D., Talchabhadel, R. and Chen, Y. (2020d) How Accurately Can Satellite Products (TMPA and IMERG) Detect Precipitation Patterns, Extremities, and Drought Across the Nepalese Himalaya? *Earth and Space Science*, **7**: e2020EA001315. <https://doi.org/10.1029/2020ea001315>
- Sharma, S., Khadka, N., Nepal, B., Ghimire, S. K., Luintel, N. and Hamal, K. (2021b) Elevation Dependency of Precipitation over Southern Slope of Central Himalaya. *Jalawaayu*, **1**: 1-14.
- Shen, Y. and Xiong, A. Y. (2016) Validation and comparison of a new gauge-based precipitation analysis over mainland China. *International Journal of Climatology*, **36**: 252-265. 10.1002/joc.4341
- Shige, S., Yamamoto, T., Tsukiyama, T., Kida, S., Ashiwake, H., Kubota, T., Seto, S., Aonashi, K. and Okamoto, K. (2009) The GSMaP Precipitation Retrieval Algorithm for Microwave Sounders-Part I: Over-Ocean Algorithm. *Ieee Transactions on Geoscience and Remote Sensing*, **47**: 3084-3097.

- Shrestha, D. and Deshar, R. (2014) Spatial Variations in the diurnal pattern of precipitation over Nepal Himalayas. *Nepal Journal of Science and Technology*, **15**: 57-64.
- Shrestha, D., Sharma, S., Hamal, K., Jadoon, U. K. and Dawadi, B. (2021) Spatial Distribution of Extreme Precipitation Events and Its Trend in Nepal. *Environmental Sciences*, **9**: 58-66.
- Shrestha, M. L. (2000) Interannual variation of summer monsoon rainfall over Nepal and its relation to Southern Oscillation Index. *Meteorology and Atmospheric Physics*, **75**: 21-28. 10.1007/s007030070012
- Sun, Q. H., Miao, C. Y., Duan, Q. Y., Ashouri, H., Sorooshian, S. and Hsu, K. L. (2018) A Review of Global Precipitation Data Sets: Data Sources, Estimation, and Intercomparisons. *Reviews of Geophysics*, **56**: 79-107.
- Sungmin, O., Foelsche, U., Kirchengast, G., Fuchsberger, J., Tan, J. and Petersen, W. A. (2017) Evaluation of GPM IMERG Early, Late, and Final rainfall estimates using WegenerNet gauge data in southeastern Austria. *Hydrology and Earth System Sciences*, **21**: 6559-6572.
- Talchabhadel, R. and Karki, R. (2019) Assessing climate boundary shifting under climate change scenarios across Nepal. *Environmental Monitoring and Assessment*, **191**: 520. <https://doi.org/10.1007/10661-019-7907-0>.
- Talchabhadel, R., Karki, R., Thapa, B. R., Maharjan, M. and Parajuli, B. (2018) Spatio-temporal variability of extreme precipitation in Nepal. *International Journal of Climatology*, **38**: 4296-4313. <https://doi.org/10.1002/joc.5669>
- Tan, J., Petersen, W. A., Kirstetter, P. E. and Tian, Y. D. (2017) Performance of IMERG as a Function of Spatiotemporal Scale. *Journal of Hydrometeorology*, **18**: 307-319. 10.1175/Jhm-D-16-0174.1
- Tang, G. Q., Ma, Y. Z., Long, D., Zhong, L. Z. and Hong, Y. (2016) Evaluation of GPM Day-1 IMERG and TMPA Version-7 legacy products over Mainland China at multiple spatiotemporal scales. *Journal of Hydrology*, **533**: 152-167.
- Tian, Y. D. and Peters-Lidard, C. D. (2010) A global map of uncertainties in satellite-based precipitation measurements. *Geophysical Research Letters*, **37**. Artn L2440710.1029/2010gl046008
- Ushio, T., Sasashige, K., Kubota, T., Shige, S., Okamoto, K., Aonashi, K., Inoue, T., Takahashi, N., Iguchi, T., Kachi, M., Oki, R., Morimoto, T. and Kawasaki, Z. I. (2009) A Kalman Filter Approach to the Global Satellite Mapping of Precipitation (GSMaP) from Combined Passive Microwave and Infrared Radiometric Data. *Journal of the Meteorological Society of Japan*, **87a**: 137-151.
- Viviroli, D., Archer, D. R., Buytaert, W., Fowler, H. J., Greenwood, G. B., Hamlet, A. F., Huang, Y., Koboltschnig, G., Litaor, M. I., Lopez-Moreno, J. I., Lorentz, S., Schadler, B., Schreier, H., Schwaiger, K., Vuille, M. and Woods, R. (2011) Climate change and mountain water resources: overview and recommendations for research, management and policy. *Hydrology and Earth System Sciences*, **15**: 471-504. 10.5194/hess-15-471-2011
- Viviroli, D., Durr, H. H., Messerli, B., Meybeck, M. and Weingartner, R. (2007) Mountains of the world, water towers for humanity: Typology, mapping, and global significance. *Water Resources Research*, **43**. Artn W0744710.1029/2006wr005653
- Viviroli, D. and Weingartner, R. (2004) The hydrological significance of mountains: from regional to global scale. *Hydrology and Earth System Sciences*, **8**: 1016-1029.
- Wang, Z. L., Zhong, R. D., Lai, C. G. and Chen, J. C. (2017) Evaluation of the GPM IMERG satellite-based precipitation products and the hydrological utility. *Atmospheric Research*, **196**: 151-163.
- Yamamoto, M. K., Ueno, K. and Nakamura, K. (2011) Comparison of Satellite Precipitation Products with Rain Gauge Data for the Khumb Region, Nepal Himalayas. *Journal of the Meteorological Society of Japan*, **89**: 597-610. 10.2151/jmsj.2011-601

- Yatagai, A. and Kawamoto, H. (2008) Quantitative estimation of orographic precipitation over the Himalayas by using TRMM/PR and a dense network of rain gauges. *Remote Sensing and Modeling of the Atmosphere, Oceans, and Interactions Ii*, **7148**. Artn 71480c  
10.1117/12.811943
- Yuan, F., Zhang, L. M., Soe, K. M. W., Ren, L. L., Zhao, C. X., Zhu, Y. H., Jiang, S. H. and Liu, Y. (2019) Applications of TRMM- and GPM-Era Multiple-Satellite Precipitation Products for Flood Simulations at Sub-Daily Scales in a Sparsely Gauged Watershed in Myanmar. *Remote Sensing*, **11**.
- Zhao, H. G., Yang, B. G., Yang, S. T., Huang, Y. C., Dong, G. T., Bai, J. and Wang, Z. W. (2018) Systematical estimation of GPM-based global satellite mapping of precipitation products over China. *Atmospheric Research*, **201**: 206-217.



© 2020 by the authors. Submitted for possible open access publication under the terms and conditions of the Creative Commons Attribution 4.0 International (CC BY) (<http://creativecommons.org/licenses/by/4.0/>).